Filamentary Instability of a Relativistic Electron Beam*

Kim Molvig
Physics Department, University of California, Irvine, California 92664, and
Research Laboratory of Electronics, Massachusetts Institute of Technology, Cambridge, Massachusetts 02139
(Received 2 September 1975)

The transverse electromagnetic or filamentary instability is reconsidered in light of recent experiments which were unable to suppress the instability by increasing the beam transverse temperature. I find that only the applied magnetic field can stabilize the mode. While the beam temperature can cause stabilization in a collisionless, $\nu=0$, plasma, for finite ν the beam is unstable to filamentation if $\omega_{pb}^2\beta^2\gamma > \Omega_{ce}^2$, regardless of its temperature.

One of the most deleterious instabilities for intense electron-beam propagation is the so-called filamentary instability.[1-4] It is a manifestation of the attractive Biot-Savart current-current interaction between beam particles which can predominate over the dynamics when the background plasma shields out the electrostatic interaction. Generally, a medium whose interparticle force is repulsive ($g>0$) undergoes oscillations at a frequency $\omega=(4\pi n g)^{1/2}$ (n is the particle density and g the coupling constant), while for an attractive ($g<0$) interparticle force the medium is unstable to density perturbations with growth $\omega_i=(4\pi n|g|)^{1/2}$. For example, g equals e^2/m for plasma oscillations, $-Gm$ for gravitational collapse, and $-e^2\beta^2/m$ for filamentation. The Biot-Savart interaction acts transversely to the velocity and so causes a filamentary structure in the electron beam.

A variety of related instabilities have been studied[5-11]; in particular I cite a computer simulation by Lee and Lampe.[11] They investigate the nonlinear evolution of well-developed beam filaments in detail, and accordingly consider only abbreviated linear theories. This Letter reports a comprehensive linear theory, resolving the previously unexplained experimental[4] observation that filamentation could not be suppressed by an increase of beam temperature. For the parameters of present-day intense-beam experiments I find an analytic expression for the growth rate which is new, Eq. (14), and in no way resembles the result of cold-fluid theory [compare Eq. (8), also Refs. 4 and 11]. Specifically, the growth rate, being proportional to the collision frequency in the background plasma, is typically 1 to 3 orders of magnitude smaller than the cold-fluid result.

We will consider a beam propagating along a magnetic guide field in a charge- and current-neutralized equilibrium. The return current is carried by plasma electrons with equilibrium drift velocity $v_e=-(n_b/n_p)v_b$, and the ions are immobile. The perturbation is perpendicular to $\vec{B}$ and the electric field polarization "ordinary," $\vec{E}\parallel\vec{B}$, as is usual for a Weibel-type[5] instability. For a nonrelativistic beam and collisionless plasma, these restrictions on the disturbance are sufficient to decouple the zz component of the dielectric tensor (cross terms due to zero-order streaming of the beam and plasma exactly cancel). In general this does not happen, although for cases of practical interest it remains true to a good approximation. Thus $D_{zz}=0$ describes the mode until third order in $\epsilon\sim\omega/kc \sim(n_b/n_p)^{1/2}$ (v_b assumed to be of order c). The wavelengths considered are sufficiently long that finite-Larmor-radius effects in the plasma are negligible. We therefore use a cold-fluid description for the plasma, incorporating collisions. The plasma contribution to D_{zz} is then simply

$$D_{zz}^{\,p}=-\omega_p^{\,2}/\omega(\omega+i\nu). \qquad (1)$$

The beam's response is calculated in its rest frame where it is assumed to be nonrelativistic $[(\Delta v/c)^2\ll 1]$ and then transformed to the lab frame. This is considerably less restrictive than the two-mass-approximation Vlasov equation, which requires $2\Delta v_\parallel/c\ll 1$. The transformation of the frequency results in a nonzero $k_\parallel$ in the beam frame, but the effects of this are of order $(\Delta v_\parallel/c)^2$, and are negligible, as is consistent with the nonrelativistic approximation. In the following we use primed quantities to denote the beam frame, and unprimed quantities to denote the lab frame.

By use of the Lorentz transformation, Faraday's law, and the continuity equation, a transformation law for the conductivity tensor is easily obtained. It takes the form

$$\overleftrightarrow{\sigma}(\vec{k},\omega)=\gamma[(\omega-\vec{k}\cdot\vec{v})/\omega]\overleftrightarrow{T}\cdot\overleftrightarrow{\sigma}'(\vec{k}',\omega')\cdot\overleftrightarrow{T}^T, \qquad (2)$$

where

$$\overleftrightarrow{T}=\overleftrightarrow{I}-\frac{\vec{v}\vec{v}}{v^2}+\frac{\vec{v}\vec{v}}{v^2}\frac{\omega-\gamma\vec{v}\cdot\vec{k}}{\gamma(\omega-\vec{k}\cdot\vec{v})}+\frac{\vec{v}\vec{k}}{\omega-\vec{k}\cdot\vec{v}} \qquad (3)$$

and $\overleftrightarrow{T}^T$ denotes the transposed matrix. For example, the beam frame is usually chosen so that the conductivity components σ_{xz}, σ_{zx}, σ_{yz}, and σ_{zy} vanish. This happens for a Vlasov beam and a two-temperature Maxwellian distribution with or without a magnetic field. Equation (2) then gives (taking $\vec{k}=k\vec{e}_x$)

$$\overleftrightarrow{\sigma}=\gamma\begin{pmatrix}\sigma_{xx}' & \sigma_{xy}' & (vk/\omega)\sigma_{xx}' \\ \sigma_{yx}' & \sigma_{yy}' & (vk/\omega)\sigma_{yx}' \\ (vk/\omega)\sigma_{xx}' & (vk/\omega)\sigma_{xy}' & \gamma^{-2}\sigma_{zz}'+(v^2k^2/\omega^2)\sigma_{xx}'\end{pmatrix}. \qquad (4)$$

The components of $\overleftrightarrow{\sigma}'$ are given in terms of the beam-frame frequency and wave vector, ω' and k'. These are transformed to the lab frame by

$$\omega'=\gamma\omega,\quad k'=k, \qquad (5)$$

consistent with our neglect of $k_{\parallel}'$.

The required beam conductivity component $\sigma_{zz}{}^b$ is obtained from Eq. (4) by use of well-known results. For this, the beam-frame beam density is given by $n_b'=n_b/\gamma$ and thus,

$$\sigma_{zz}{}^b=-\frac{i}{4\pi}\frac{\omega_b{}^2}{\gamma}e^{-\lambda}\left[\frac{1}{\gamma^2}\sum_{n=-\infty}^{+\infty}I_n(\lambda)\left(\frac{1}{\omega}-\frac{T_\parallel}{T_\perp}\frac{n\Omega}{\gamma\omega}\frac{1}{n\Omega/\gamma+\omega}\right)-\frac{v^2k^2}{\omega^2}\sum_{n=-\infty}^{+\infty}\frac{n^2}{\lambda}\frac{I_n(\lambda)}{n\Omega/\gamma+\omega}\right], \qquad (6)$$

where $\Omega\equiv|eB/mc|$, $\lambda\equiv k^2\kappa T_\perp/\Omega^2 m$, and $\omega_b{}^2\equiv 4\pi n_b e^2/m$ so that all γ dependence is shown explicitly. The first term in Eq. (6) must be discarded since it is two orders smaller in ω/kc than the last term. Finally, we add the plasma, beam, and Maxwell-equation contributions to the dielectric tensor, giving the dispersion relation

$$D_{zz}=\frac{k^2c^2}{\omega^2}+\frac{\omega_p{}^2}{\omega(\omega+i\nu)}+\frac{\omega_b{}^2v^2\gamma e^{-\lambda}}{\omega^2\kappa T_\perp/m}\sum_{n=1}^{\infty}\frac{2n^2\Omega^2I_n(\lambda)}{\gamma^2(\omega^2-n^2\Omega^2/\gamma^2)}=0. \qquad (7)$$

Note that only perpendicular temperature enters Eq. (7). This is to be expected since $v\sim c$ and the temperatures are nonrelativistic.

The mode does not depend on the detailed form of the beam distribution function. An identical dispersion relation can be obtained for a monoenergetic distribution with an angular spread. The nonrelativistic beam-frame temperature restriction is then replaced by $\Delta\ll 1$ (Δ is the rms angular spread), but transverse velocities can be relativistic. One may apply the results given here by using the effective temperature $T_\perp\equiv\frac{1}{2}\times mv^2\gamma^2\Delta^2$.

For wavelengths much greater than the beam electron Larmor radius, Eq. (7) may be expanded in powers of λ. To lowest order, the result coincides with that obtained from cold-fluid equations,

$$\omega^2=\frac{\Omega^2}{\gamma^2}-\frac{\omega_b{}^2\beta^2}{\gamma}\left[1+\frac{\omega_p{}^2}{k^2c^2(1+i\nu/\omega)}\right]^{-1}. \qquad (8)$$

For strongly unstable cases, $\omega_b{}^2\beta^2>\Omega^2/\gamma$, this equation will usually apply to long wavelengths. Increasing k eventually invalidates the small-λ expansion, however, so that Eq. (8) does not apply to the shortest wavelengths. The next-order corrections differ in form from the fluid equations with thermal corrections.[4] In any case, the finite-Larmor-radius effects, which eventually stabilize the mode at large k, require most of the series in (7) for an adequate description.

For the purely growing mode we seek, it is convenient to use the dimensionless frequency variable $x\equiv-i\omega\gamma/\Omega$. With scaling of ν to Ω/γ also, Eq. (7) becomes

$$C_M\lambda+C_T\frac{x}{\nu+x}=2e^{-\lambda}\sum_{n=1}^{\infty}n^2I_n(\lambda)\frac{1}{x^2+n^2}, \qquad (9)$$

where

$$C_M\equiv\Omega^2/\omega_b{}^2\beta^2\gamma,\quad C_T\equiv\omega_p{}^2v_T{}^2/\omega_b{}^2\beta^2\gamma c^2 \qquad (10)$$

are the coefficients characterizing field strength and beam temperature.

Equation (9) has solutions which are discontinuous at $\nu=0$, so that its collisionless version gives incorrect results for an actual physical system. To point out the difference caused by a finite collision frequency, I state without derivation the collisionless results.

The roots obtained correspond to pure oscillations or growth with (at most) one unstable mode. This mode can be stabilized by either magnetic field or temperature, independently. Crude, though sufficient, conditions for stability of all wavelengths are

$$\Omega^2 > \omega_b^2 \beta^2 \gamma \tag{11}$$

for magnetic-field stabilization ($C_M > 1$), and

$$\omega_p^2 v_T^2 / c^2 > \omega_b^2 \beta^2 \gamma \tag{12}$$

for beam-temperature stabilization ($C_T > 1$). Condition (11) can also be obtained from the cold-fluid theory.[10,11] Condition (12) is equivalent to the Bennett[12] pinch condition as is familiar[6] in the related anisotropic temperature instability.[5]

Beam temperature can stabilize the mode only at $\nu = 0$. For finite ν the stability condition is simply given by Eq. (11) and this is precise, i.e., both necessary and sufficient. Thus, when $\nu > 0$, the dispersion relation has a purely growing root if (11) fails ($C_M < 1$). This follows from an inequality which holds when $C_M < 1$:

$$C_M \lambda < 2e^{-\lambda} \sum_{n=1}^{\infty} I_n(\lambda) \text{ for } 0 \leq \lambda \leq \lambda_{\max}. \tag{13}$$

The inequality may be verified by summing the series to give the right-hand side of (13) as $1 - e^{-\lambda} I_0(\lambda)$, which goes like λ for λ small but approaches 1 as $\lambda \to \infty$. Now since the left-hand side of (9) increases monotonically from $C_M \lambda$ to $C_M \lambda + C_T$ as x goes from 0 to ∞ and the right-hand side of (9) decreases from $2e^{-\lambda} \sum_n I_n(\lambda)$ ($n = 1$ to ∞) to zero over the same interval of x, (13) implies that (9) is satisfied for some positive x when $0 < \lambda < \lambda_{\max}$. The sufficiency of (11) can be shown similarly by allowing x to be complex in Eq. (9) and considering its real part. It then becomes clear that $C_M > 1$ prohibits any solutions of Eq. (9) for Re$x > 0$.

These various points are borne out in Fig. 1 which gives a numerical evaluation of the growth rates. The case shown illustrates the effect of collisions. Actual experiments[1-4] are presently conducted in a different regime where the temperature parameter C_T is quite large, typically 10. In this case, the instability exists only because of collisions, and the growth rate is correspondingly small. When $\nu < \Omega$, we will have $x^2 \ll 1$ so that the series in (9) may be summed to give the

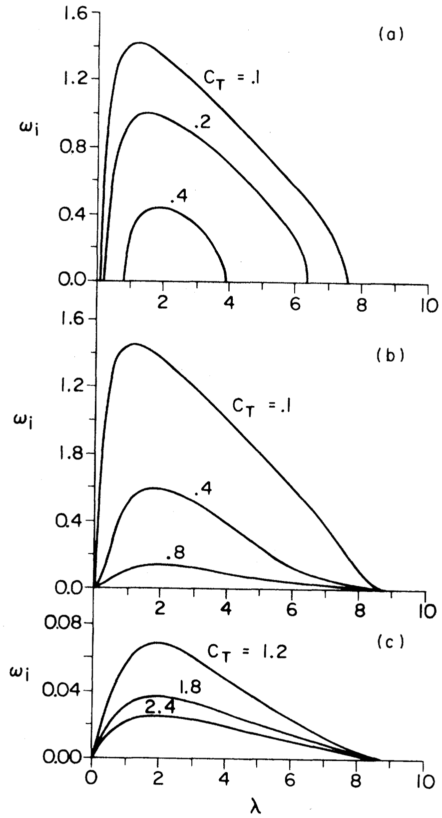

FIG. 1. Growth rates versus λ. Frequency units are Ω/γ and $C_M = 0.1$. For (a), $\nu = 0$. At $C_T = 0.6$, the mode is stable. For (b) and (c), $\nu = 0.1$. (c) has an expanded vertical scale, showing medium values of C_T. At larger C_T values (or lower ν), the analytic expression Eq. (14) is applicable.

growth rate for resistive filamentation,

$$\omega_i = \nu \frac{\omega_b^2 \beta^2 \gamma}{\omega_p^2} \frac{c^2}{v_T^2} [1 - e^{-\lambda} I_0(\lambda) - C_M \lambda]. \tag{14}$$

As an example with $\nu \sim 2 \times 10^9$, $n_b \sim 10^{12}$, $n_p \sim 10^{14}$, $\kappa T_\perp \sim 50$ keV, $\beta^2 \gamma \sim 1$, and $B_0 \sim 1$ kG, Eq. (14) gives a maximum growth at $\lambda \sim 2$ of about $\omega_i \sim 10^8$. [Equation (8) gives $\omega_i \sim \omega_b \sim 6 \times 10^{10}$, or a discrepancy of almost 3 orders of magnitude.] Growth rates have not been measured precisely but are certainly much larger. Consistency with experiment[4] would require a collision frequency on the order of 2×10^{10}. This supports the existence of an extremely anomalous collision frequency accompanying intense beam propagation. A similar conclusion has been drawn from experiments at Physics International Company[13] but for different reasons.

In conclusion, when temperature and collisional effects are accounted for, the filamentary instability can be stabilized by the applied magnetic field only. Beam–transverse-temperature stabilization, according to the Bennett pinch condition, Eq. (12), does not occur because of a finite resistivity in the background plasma. In present experimental regimes, the mode is of the resistive type.

I would like to thank Gregory Benford, C. W. Roberson, and Norman Rostoker for many useful discussions.

*Work supported in part by U. S. Energy Research and Development Administration Contracts No. AT(04-3)34 PA207 (University of California, Irvine) and No. EA(11-1)-3070 (Massachusetts Institute of Technology).

[1]G. Yonas and P. Spence, Physics International Co. Report No. PIFR-106, 1968 (unpublished).

[2]P. W. Spence, B. Ecker, and G. Yonas, Bull. Am. Phys. Soc. 14, 1007 (1969).

[3]C. Stallings, Physics International Co. Report No. PIFR-366, 1972 (unpublished).

[4]C. A. Kapetanakos, Appl. Phys. Lett. 25, 484 (1974).

[5]E. S. Weibel, Phys. Rev. Lett. 2, 83 (1959).

[6]H. P. Furth, Phys. Fluids 6, 48 (1963).

[7]S. Hamasaki, Phys. Fluids 11, 1173, 2724 (1968).

[8]M. Bornatici and K. F. Lee, Phys. Fluids 13, 3007 (1970).

[9]K. F. Lee and J. C. Armstrong, Phys. Rev. A 4, 2087 (1971).

[10]G. Benford, Phys. Rev. Lett. 28, 1242 (1972), and Plasma Phys. 15, 483 (1973).

[11]R. Lee and M. Lampe, Phys. Rev. Lett. 31, 1390 (1973).

[12]W. H. Bennett, Phys. Rev. 45, 890 (1934).

[13]D. Prono, B. Ecker, N. Bergstrom, J. Benford, and S. Putnam, Physics International Co. Report No. PIFR-557, 1975 (unpublished).

Impurity Transport in a Quiescent Tokamak Plasma*

S. A. Cohen, J. L. Cecchi, and E. S. Marmar
Plasma Physics Laboratory, Princeton University, Princeton, New Jersey 08540
(Received 14 July 1975)

We have injected short bursts of aluminum into the adiabatic-toroidal-compressor (ATC) tokamak, and measured the time evolution of the radial distribution of highly ionized states of aluminum. The results are compared with a computer code describing neoclassical impurity diffusion.

The transport of high-Z ions in tokamak plasmas is of crucial importance because impurity profiles greatly affect radiation losses,[1] reactivity,[2] and stability,[3] as well as the efficacy of the various heating schemes.[4] Considerable efforts have been made to measure intrinsic impurity content[5,6] and profiles.[7,8] However, it is difficult to determine transport coefficients from these experiments because of the lack of knowledge of the impurity source function. By employing a new impurity injection technique[9] in conjunction with vacuum ultraviolet (VUV) spectroscopy, we have been able to measure the radial transport of aluminum ions in a dirty ($Z_{eff}=4.6$),[10] quiescent (no large kinklike modes), tokamak plasma. The measurements have been compared with a computer code describing Pfirsch-Schlüter impurity diffusion[11] and agreement is found. We consider this to be further evidence of the neoclassical behavior of ions in tokamaks.

The details of the impurity injection technique have been described elsewhere.[9] High-power laser irradiation of an aluminized glass slide produces a 300-μsec burst containing $\sim 5\times10^{16}$ neutral aluminum atoms with ~ 3 eV mean energy. These atoms are directed into the adiabatic-toroidal-compressor (ATC) tokamak, in which the total number of electrons is approximately 10^{19}. The injected aluminum atoms penetrate about 2 cm into the plasma before being ionized to Al II. The ionization process continues as the ions rapidly circulate along the field lines and, less rapidly, move across them. The time evolution of the line integral of the emissivity for different aluminum ionization states is measured using an absolutely calibrated, grazing-incidence VUV monochromator (McPherson Model No. 247). Observations are made of the strong $\Delta n=0$ transitions to the ground state ($\lambda=278.7$, 309.6, 352.2, 388.0, 385.0, 332.8, and 550.01 Å for Al V, VI, VII, VIII, IX, X, and XI, respectively).

During these experiments magnetic probes showed that no large magnetohydrodynamic kinklike modes were present and that the up-down and in-out stability was ±1.0 cm. With use of a 4-mm microwave interferometer the average